# Seasonal Behavior of Tropical to Mid-Latitude Upper Tropospheric Water Vapor from UARS MLS

Brad J. Sandor[1,2], William G. Read[1], Joe W. Waters[1], Karen H. Rosenlof[3]

Received _____; accepted _____

Short title:

[1]Jet Propulsion Laboratory, California Institute of Technology, Pasadena

[2]Now at National Center for Atmospheric Research, Boulder, CO

[3]Cooperative Institute for Research in Environmental Sciences and NOAA Aeronomy Laboratory, Boulder, CO

# 1. Introduction

Upper tropospheric humidity (UTH) is of fundamental importance in understanding Earth's atmosphere and climate. Water vapor is the most important greenhouse gas [*Manabe and Wetherald*, 1967; *Jones and Mitchell*, 1991] and it is in the upper troposphere that water vapor most strongly influences radiative forcing [*Udelhofen and Hartmann*, 1994]. Surface warming due to anthropogenic increases in $CO_2$ and other greenhouse gases is expected to occur with relative humidity remaining approximately constant, implying an increase in absolute humidity and consequent positive feedback to global warming [*Manabe and Wetherald*, 1967]. A representative modeling result [*Rind et al.*, 1991] is that water vapor feedback contributes ~40% of the global-average surface temperature increase in a doubled-$CO_2$ climate. An alternative scenario has been proposed [*Lindzen*, 1990] in which the increased convective activity due to $CO_2$ warming will dry the upper troposphere by shifting detrainment of air from convective plumes to a higher (colder) altitude and converting more vapor to precipitation, thereby enhancing subsidence and providing a negative feedback to global warming. Satellite solar occultation observations of higher zonal mean summer than winter UTH values have been cited as evidence that enhanced convection moistens the upper troposphere [*Rind et al.*, 1991]. However, *Pierrehumbert* [1995] has argued that, due to the nonlinear dependence of outgoing longwave radiation (OLR) on UTH, zonal mean UTH is less important for radiative forcing than the dryness of, and prevalence of, the driest tropical UTH values. The importance of this issue is emphasized by observations of tropical 300-500 hPa UTH that show the peak of the UTH frequency distribution is drier during the time of strongest convection (July) than the time of weakest convection (January) [*Spencer and Braswell*, 1997; *Chiou et al.*, 1997]. Despite the importance of UTH, uncertainties in current values lead to uncertainties in calculated outgoing infrared flux from the troposphere comparable in magnitude to the change in outgoing IR flux calculated for a doubled $CO_2$ atmosphere [*Gutzler*, 1993]. Accurate measurements of upper tropospheric

restricted to pressures greater than 300 hPa by instrumental limitations, and are sparse in remote oceanic regions. Advantages of high vertical resolution, near global coverage with 1300 profiles per day, and relative insensitivity to aerosol (cirrus and volcanic) contamination make MLS a valuable new system for measuring UTH.

MLS UTH initial observations and retrieval techniques are described by *Read et al.* [1995], who also present preliminary scientific results at 215 hPa. *Read et al.* [1995] demonstrate the usefulness of MLS UTH observations for measurements of zonal mean behavior, tracking large-scale weather systems, and mapping seasonal behavior on 4°×4° horizontal scales. More detailed study of 215 hPa zonal mean behavior is presented by *Elson et al.* [1996], in parallel with a similar study of stratospheric water vapor. *Stone et al.* [1996] present a case study of baroclinic wave activity from its signature in the 215 hPa MLS UTH data.

In the current study, initial results of an improved retrieval scheme for MLS UTH are described. Zonal-mean global MLS UTH measurements from a five-year data set are analyzed for seasonal variability on 316, 215, and 147 hPa pressure surfaces and tropical to mid- latitudes, and discussed in the context of lower altitude TOVS [*Soden and Bretherton*, 1996] and higher altitude HALOE [*Rosenlof et al.*, 1997] data. Monthly frequency distributions of UTH values are presented for 30°S- 30°N on these pressure levels, and compared with lower altitude UTH frequency distributions [*Spencer and Braswell*, 1997; *Chiou et al.*, 1997].

## 2. Observations

The initial MLS UTH retrieval described by *Read et al.* [1995] has been improved by using better characterization of the dry and wet absorption continua, and including field of view and refractive effects, combined with an iterated optimal estimation retrieval. This new retrieval [*Read et al., manuscript in preparation*], which will produce the MLS Version 4 data product for public use in 1998, provides UTH on 464, 316, 215, and 147

more slowly with altitude than does mixing ratio, interpolation between measurements in $RH_i$ units provides a more accurate profile shape.

$RH_i$ units are most appropriate for low and mid latitudes, but for the MLS retrieval have the disadvantage of de-emphasizing latitudes higher than ~50°, where all three pressure surfaces are usually in the lower stratosphere [*Holton et al.*, 1995; *Appenzeller et al.*, 1996]. Retrieved $H_2O$ mixing ratios in these regions are very low, and the dependence of mixing ratio on altitude is relatively weak, consistent with stratospheric behavior. In the present work, zonal mean relative humidities less than ~5% are not discussed, and this is the determining factor in the high latitude cut-offs of the data presentation. In cases involving high latitude studies, mixing ratio units may be preferred. Mixing ratio or relative humidity with respect to liquid ($RH_l$) are preferred when making comparison with data sets reported in those units, and are readily obtained from MLS $RH_i$ values with use of coincident temperatures.

As a preliminary validation of the MLS data, figures 1 and 2 present comparisons with balloon sonde [*Elliott and Gaffen*, 1991; *Larsen et al.*, 1993] and SAGE II [*Chiou et al.*, 1997] data, respectively. Sonde measurements are from a global network of 2-4 times daily balloon launches at land-based meteorological stations. Figure 1 presents the average of MLS and sonde measurements from the 62 days for which Version 4 data are available, where those measurements are coincident within 2° latitude, 2° longitude, and 3 hours time. MLS retrieved values greater than 100% (which occur only in the 0°-20°N, 147 hPa bin of figure 1) have been set to 100% for comparison as a way to account for ice contamination. Sonde measurements are least accurate in the cold, dry conditions typical of the upper troposphere, and display systematic biases among instrument types. To minimize these problems, figure 1 includes sonde data from a single instrument type, the thin film capacitor, chosen because it is the instrument type most reliable in the upper troposphere [eg *Larsen et al.*, 1993]. Figure 1 shows MLS to be consistently drier than sonde measurements at 316 and 464 hPa. Sensitivity studies to date indicate

seen in lower stratospheric water vapor [*Rosenlof et al.*, 1997]. In section 4, monthly frequency distributions are presented for tropical (30°S-30°N) latitudes, and compared with microwave (183 GHz) nadir-looking observations made with the Special Sensor Microwave humidity sounder (SSM/T-2) at lower altitudes [*Spencer and Braswell*, 1997], and with the *Chiou et al.* [1997] frequency distribution analysis of SAGE II UTH data.

## 3. Zonal Mean Seasonal Behavior

UTH measurements from the September 1991 start of the UARS mission to June 1997 are presented in figure 3 for pressure levels 147, 215, and 316 hPa. An 8-day Gaussian smoothing algorithm has been applied to suppress effects of short term variability (i.e. weather), and data have been binned by day of year to display seasonal behavior. These procedures lead to complete temporal coverage for latitudes 34°S to 34°N. The UARS satellite operations dictate that MLS alternate between observing latitudes 34°N-80°S for one ~36 day period and 34°S-80°N for the next ~36 days, resulting in periodic data gaps at latitudes poleward of 34°.

Contours of constant relative humidity shift in latitude, following the sun with a lag of about 2 months. Maximum UTH on each pressure level oscillates between approximately 10°S and 10°N, following the annual motion of the Intertropical Convergence Zone (ITCZ) associated with the ascending branch of the Hadley cell. This seasonal shifting of the ITCZ is also seen in sonde [*Peixoto and Oort*, 1996], TOVS [*Soden and Bretherton*, 1996], and SAGE [*Rind et al.*, 1993] data sets. At fixed latitudes lower than 15°, two local maxima are seen in the annual cycle, corresponding to north and south shifting of the ITCZ. The two maxima are most clear at 147 hPa for 0-10°N of the equator, where the UTH cycle is largely semi-annual (figures 3a and 4a). For latitudes higher than about 15°, a single maximum value occurs during late spring to late summer. Relative humidity values in the northern extratropics are generally higher than seasonally adjusted values at the equivalent southern extratropical latitudes (as expected from the

in stratospheric water vapor (seen in HALOE data) occurs about a month after maximum in UTH (seen in MLS data). In the tropical Southern Hemisphere the maximum in stratospheric water vapor occurs 10 months after the maximum in UTH, while the minimum in Southern Hemisphere stratospheric water vapor occurs 1-2 months after the Southern Hemisphere UTH maximum. Thus seasonal $H_2O$ maxima in the upper troposphere and lower stratosphere are nearly simultaneous at north tropical latitudes, but well separated in time at south tropical latitudes. These observations support the idea that the lower stratosphere is supplied with water directly from the upper troposphere in the Northern Hemisphere, but not in the Southern Hemisphere. The maximum entry of UTH to the stratosphere occurs at the time of maximum tropical UTH, as well as at the time of maximum tropical tropopause temperatures [*Mote et al.*, 1996].

Throughout the year, the TOVS nadir-sounding data [*Soden and Bretherton*, 1996] display 200-500 hPa UTH maxima at the ITCZ and at midlatitude storm tracks, with intervening subtropical minima 20-30° north and south of the ITCZ. MLS measures similar subtropical minima in $RH_i$ (figure 3), located 20-30° north and south of the ITCZ on the 316 and 215 hPa pressure surfaces. This structure is prevalent through the year at 316 hPa, and distinct at 215 hPa only in the northern hemisphere during May-August. It is not seen at 147 hPa, where $RH_i$ decreases monotonically with latitude from the ITCZ to midlatitudes throughout the year. The qualitative agreement between UTH behaviors seen in TOVS 200-500 hPa data and MLS 316 hPa data provides some validation of each measurement system. The MLS data at 215 and 147 hPa depict a transition away from lower altitude behavior. The absence of a subtropical minimum at 147 hPa suggests the zonal mean midlatitude convection is not deep enough to produce a secondary maximum in UTH. The seasonal behavior at 215 hPa suggests midlatitude convection is strong enough to produce a secondary UTH maximum during northern hemisphere spring-summer, in association with the seasonal maximum in solar heating. The stronger northern than southern hemisphere midlatitude secondary maximum is consistent with

quency peaks at about $RH_i$ =11% for 400-650 hPa and 20% for 450-800 hPa, with no clear difference between January and July peaks. *Chiou et al.* [1997] present a similar frequency analysis, comparing SAGE II data for DJF with JJA for 300 hPa, albeit at lower $RH_i$ resolution (~5%) than that of the SSM/T-2 analysis (1%). Equatorward of 30°, the SAGE II frequency distribution peak is at 10% in DJF, and 7.5% in JJA, similar to the SSM/T-2 January vs July 300-500 hPa result.

Figure 6 shows the monthly frequency distributions of MLS $RH_i$ values for latitudes 30°S-30°N. Values are from the years 1991-1997, and total number of measurements varies from month to month. Figure 7 shows mean, median, and mode values vs. month of year for $RH_i$ at 30°S-30°N latitude determined from the MLS measurements at 147, 215, and 316 hPa. Mean values for this latitude range are lowest at 316 hPa, highest at 215 hPa, and monthly mean values vary by less than 10% from the annual mean at each pressure level. Monthly median values follow a similar pattern. Monthly mode values are more variable, ranging from 5% to 23% at 147 hPa, and 7% to 25% at 215 hPa. The general shape of the MLS UTH frequency distributions is similar to that seen in the SSM/T-2 data [*Spencer and Braswell*, 1997] and SAGE II [*Chiou et al.*, 1997] data, in that the mode (peak) values are significantly drier than the mean and median. *Spencer and Braswell* [1997] show peak values in the frequency distributions for January and July 1994 to become drier with increasing altitude up to their highest (300-500 hPa) altitude bin. MLS UTH values show this trend continues from 316 to 147 hPa in January, but is reversed in July-August (figure 7c).

Values of the frequency distribution mode for 30°S-30°N at comparable altitudes are indistinguishable among the tropical wet (JJA) vs dry (DJF) period analyses of SSM/T-2 [*Spencer and Braswell*, 1997], SAGE II [*Chiou et al.*, 1997], and MLS [this work] data. SSM/T-2 300-500 hPa data show $RH_i$ modes of 6% in July and 9% in January; MLS 316 hPa data show $RH_i$ modes of 5% in July and 9% in January. SAGE II 300 hPa data (reported on a 5% grid) have modes 7.5% in JJA and 10% in DJF; MLS 316 hPa $RH_i$

$H_2O$ maxima in the upper troposphere and lower stratosphere are simultaneous at north tropical latitudes, but well separated in time at south tropical latitudes, consistent with the *Rosenlof et al.* [1997] hemispheric asymmetry analysis.

A UTH frequency distribution analysis of 30°S-30°N shows mode values are much drier than mean and median values, similar to nadir-sounding SSM/T-2 observations at lower altitudes [*Spencer and Braswell*, 1997], and to the 300 hPa SAGE II limb sounding data. The peak in this frequency distribution is drier in the tropical wet season (June-August) than in the tropical dry season (December-February) at 316 hPa, but wetter in the wet season than dry season at 147 hPa. Wettest values of the UTH frequency distribution peak occur in March-May, corresponding to neither the tropical wet (JJA) nor dry (DJF) periods. MLS measurements thus show the dryness and frequency distribution of the driest tropical UTH values are complex functions of altitude and season.

**Acknowledgments.** The research described in this paper was performed while B. J. Sandor held a National Research Council-NASA Resident Research Associateship award at the Jet Propulsion Laboratory, California Institute of Technology, under contract with the National Aeronautics and Space Administration.

Rind, A comparison of the Stratospheric Aerosol and Gas Experiment II tropospheric water vapor to radiosonde measurements, *J. Geophys. Res.*, *98*, 4897–4917, 1993.

Lindzen, R.S., Some coolness regarding global warming, *Bull. Am. Meteorol. Soc.*, *71*, 288–299, 1990.

Manabe, S., and R.T. Wetherald, Thermal equilibrium of the atmosphere with a given distribution of relative humidity, *J. Atmos. Sci.*, *24*, 241–259, 1967.

Mote, P.W., K.H. Rosenlof, M.E. McIntyre, E.S. Carr, J.C. Gille, J.R. Holton, J.S. Kinnersley, H.C. Pumphrey, J.M. Russell III, and J.W. Waters, An atmospheric tape recorder: The imprint of tropical tropopause temperatures on stratospheric water vapor, *J. Geophys. Res.*, *101*, 3989–4006, 1996.

Newell, R.E., Y. Zhu, E.V. Browell, S. Ismail, W.G. Read, J.W. Waters, K.K. Kelly, and S.C. Liu, Upper tropospheric water vapor and cirrus: Comparison of DC-8 observations, preliminary UARS microwave limb sounder measurements and meteorological analyses, *J. Geophys. Res.*, *101*, 1931–1941, 1996.

Peixoto, J.P., and A.H. Oort, The climatology of relative humidity in the atmosphere, *J. Climate*, *9*, 3443–3463, 1996.

Pierrehumbert, R.T., Thermostats, radiator fins, and the local runaway greenhouse, *J. Atmos. Sci.*, *52*, 1784–1806, 1995.

Read, W.G., J.W. Waters, D.A. Flower, L. Froidevaux, R.F. Jarnot, D.L. Hartmann, R.S. Harwood, and R.B. Rood, Upper tropospheric water vapor from UARS MLS, *Bull. Am. Meteorol. Soc.*, *76*, 2381–2389, 1995.

Rind, D., E.-W. Chiou, W. Chu, J. Larsen, S. Oltmans, J.Lerner, M.P. McCormick, and L. McMaster, Positive water vapor feedback in climate models confirmed by satellite data, *Nature*, *349*, 500–503, 1991.

Rind, D., E.-W. Chiou, S. Oltmans, J. Lerner, J. Larsen, M.P. McCormick, and L. McMaster, Overview of the Stratospheric Aerosol and Gas Experiment II water vapor observations: Method, validation, and data characteristics, *J. Geophys. Res.*, *98*, 4835–4856, 1993.

Rosenlof, K.H., A.F. Tuck, K.K. Kelly, J.M. Russell III, and M.P. McCormick, Hemispheric asymmetries in water vapor and inferences about transport in the lower stratosphere, *J.*

**Figure 1.** Comparison of average results of coincident balloon sonde and MLS UTH determinations from 62 days for which Version 4 MLS data have been produced. Each point shown is the average of measurements meeting coincidence criteria (see text) within a 20° latitude range. For latitude bins 40°S-20°S, 20°S-0°, 0°-20°N, and 20°N-40°N, the numbers of coincidences are 20, 5, 28, and 52, respectively.

**Figure 2.** Comparison of zonal mean SAGE II [*Chiou et al.*, 1997] and MLS UTH values for (a) 147 hPa, (b) 215 hPa, (c) 316 hPa.

**Figure 3.** Relative humidity with respect to ice on pressure surfaces at (a) 147, (b) 215, and (c) 316 hPa, as measured with the UARS MLS instrument. An 8-day Gaussian smoothing has been applied to suppress short term variability, and data from September 1991 to June 1997 averaged to determine mean seasonal behavior. The 1991-1997 average most strongly represents the first half of this time period, due to the decrease in measurement frequency associated with increasing age of UARS.

**Figure 4.** Relative humidity with respect to ice at latitudes (a) 5-10°N and (b) 5-10°S.

Fig 1: Sonde vs MLS

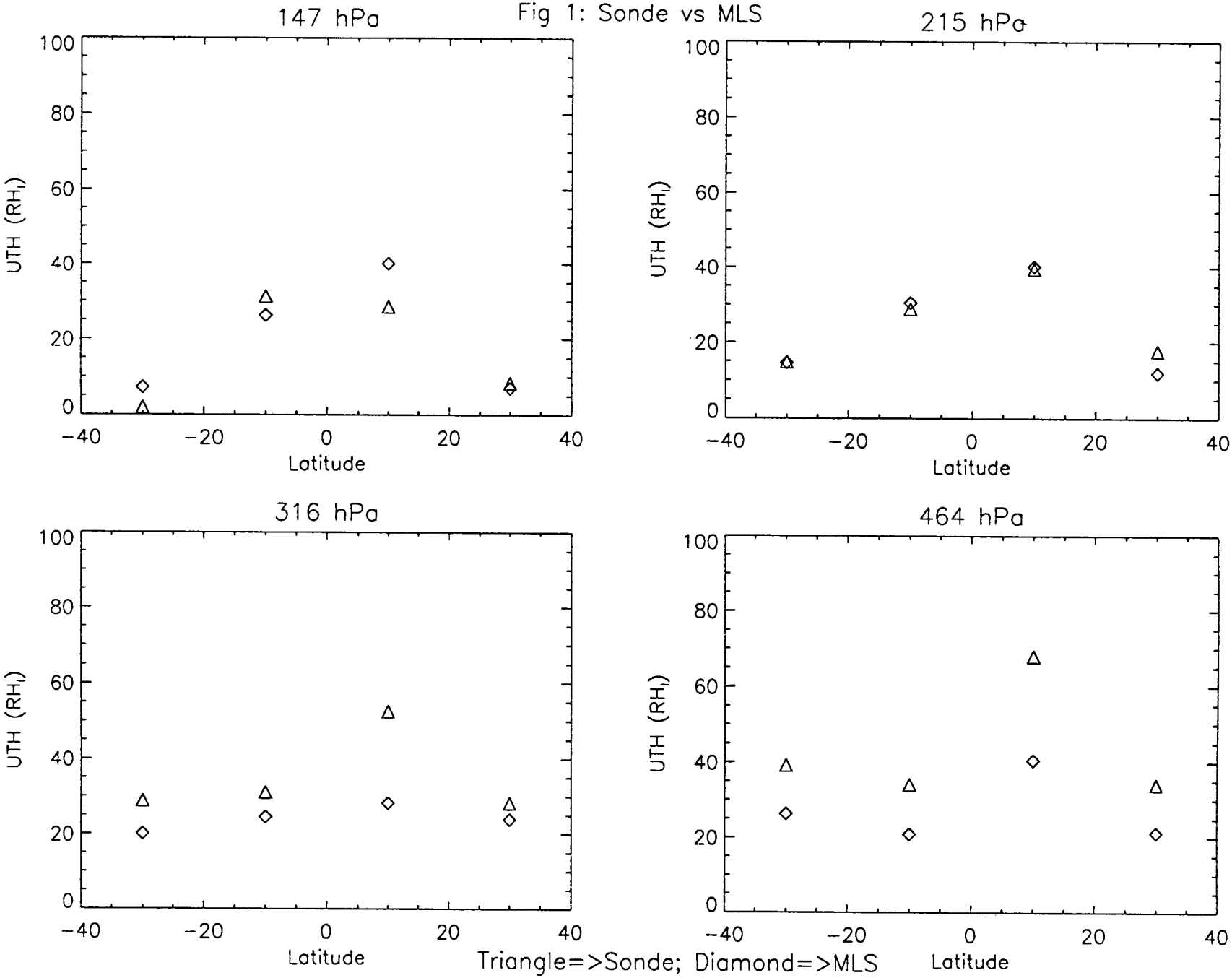

Fig 2a: 147 hPa

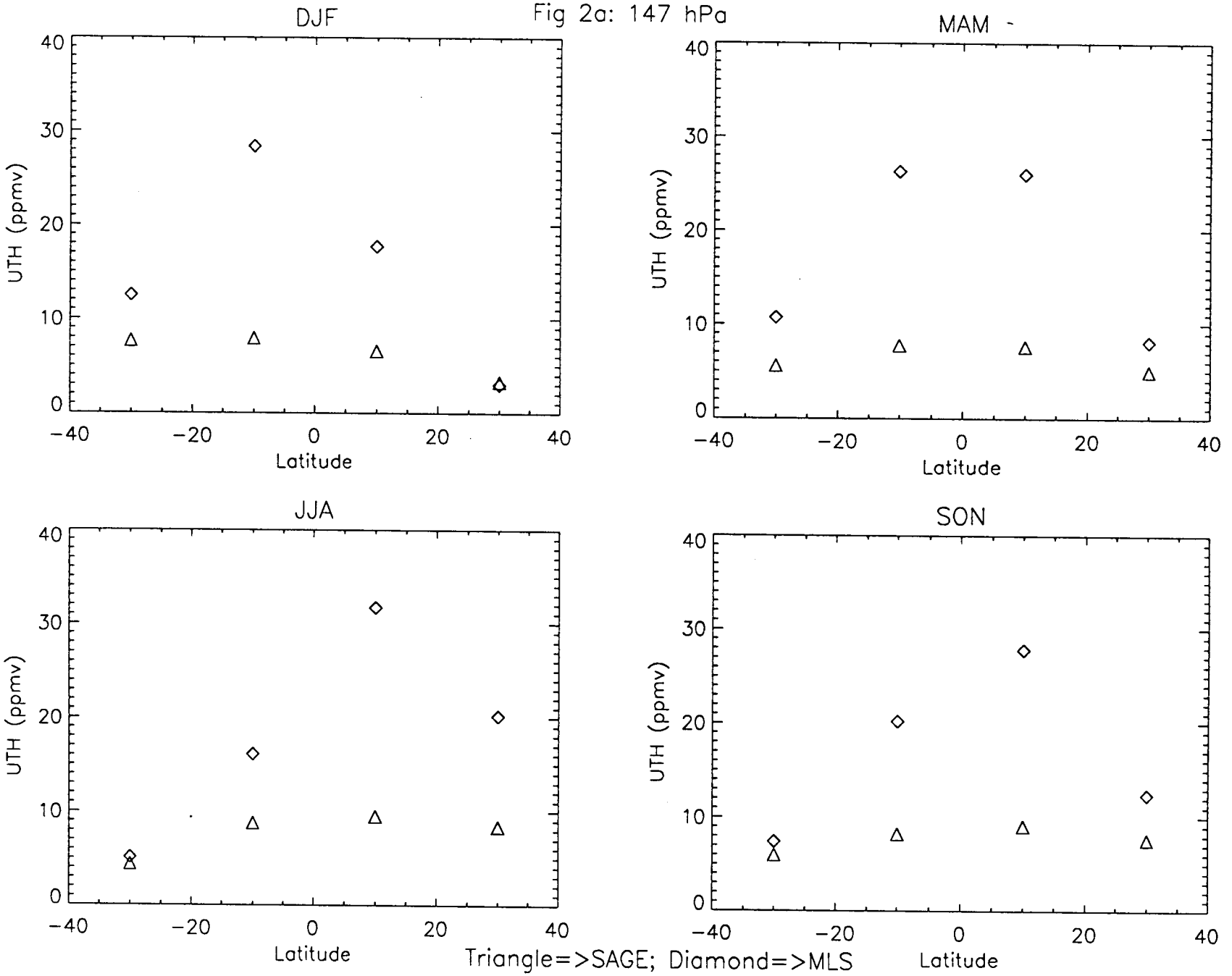

Fig 2b: 215 hPa

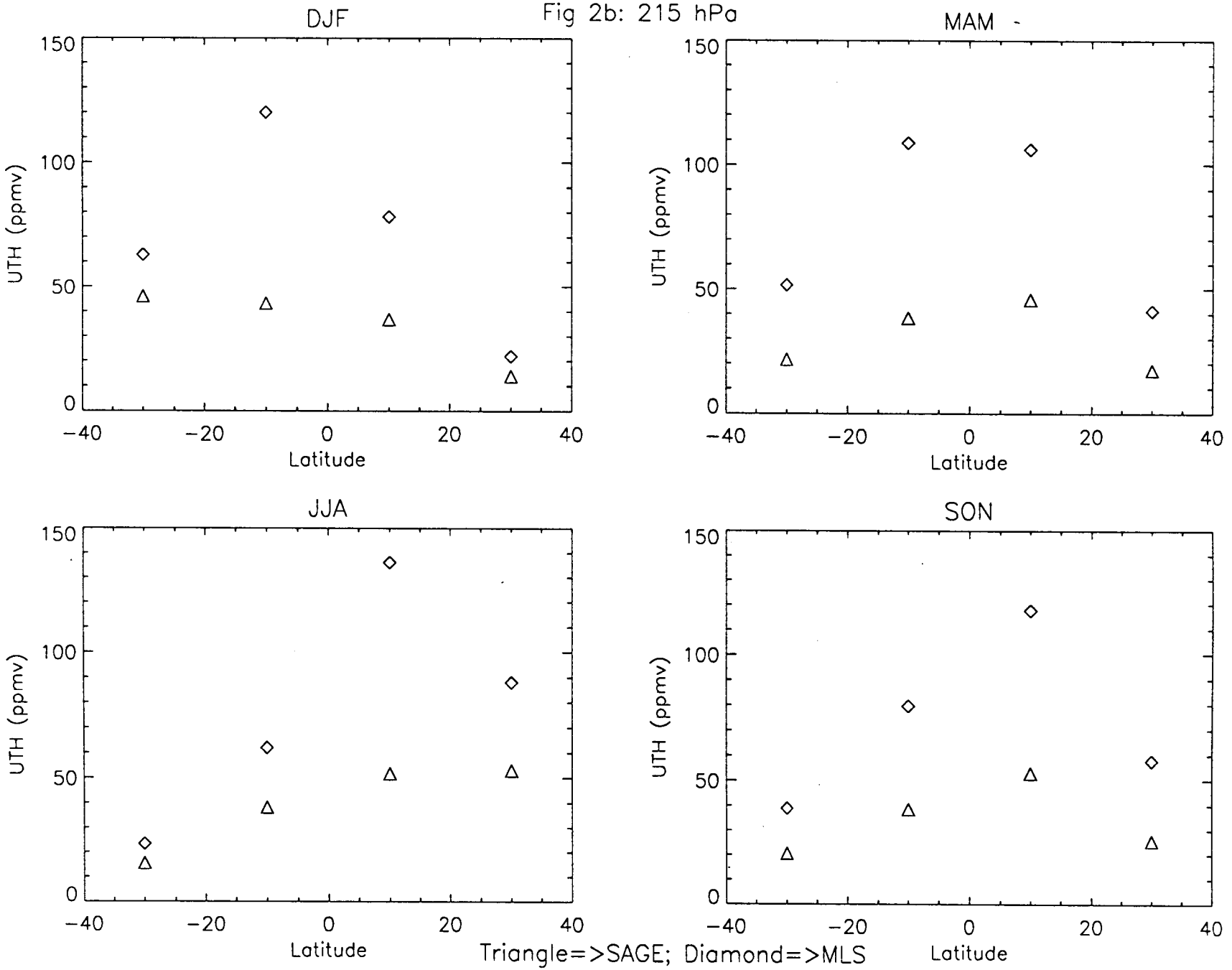

Fig 2c: 316 hPa

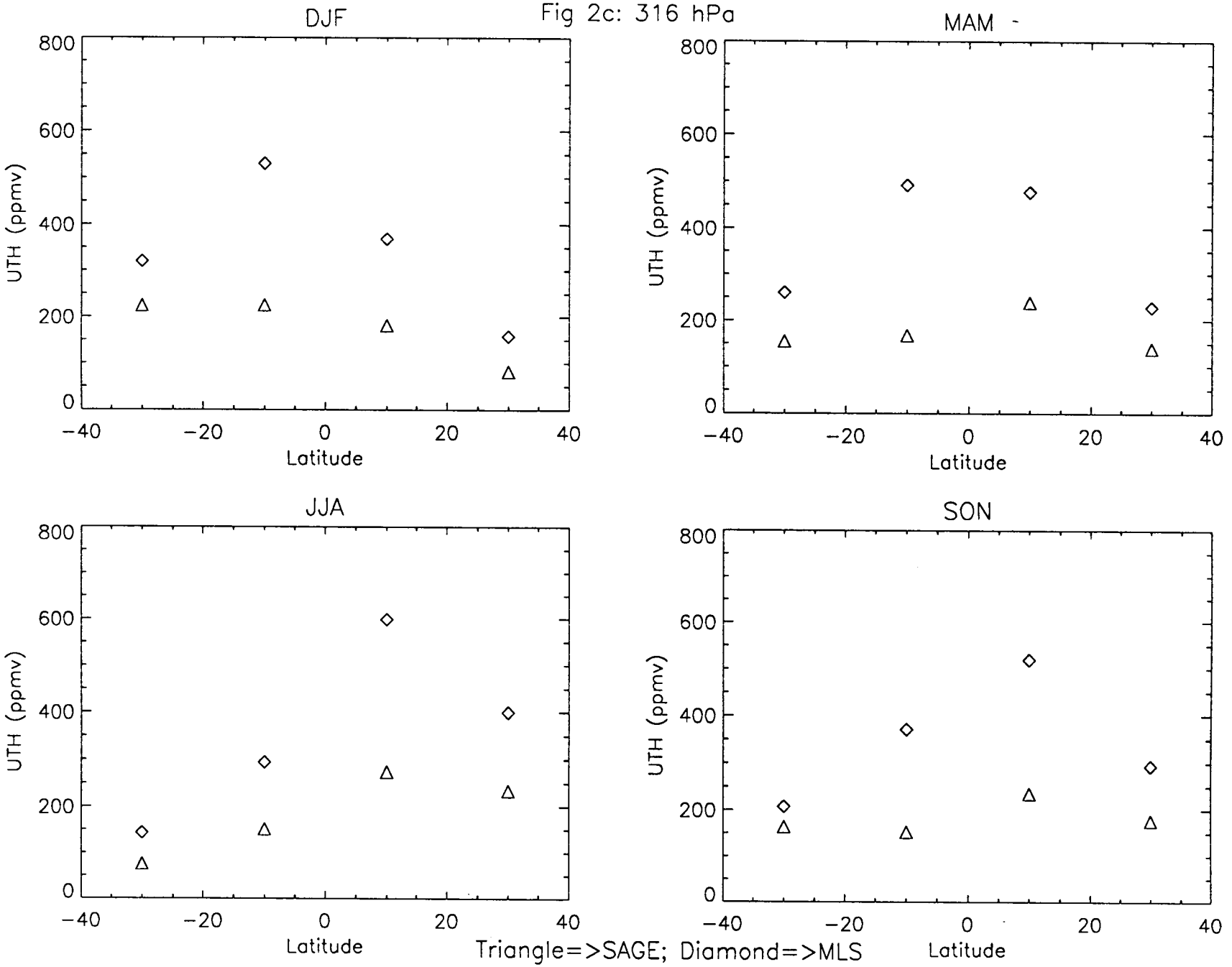

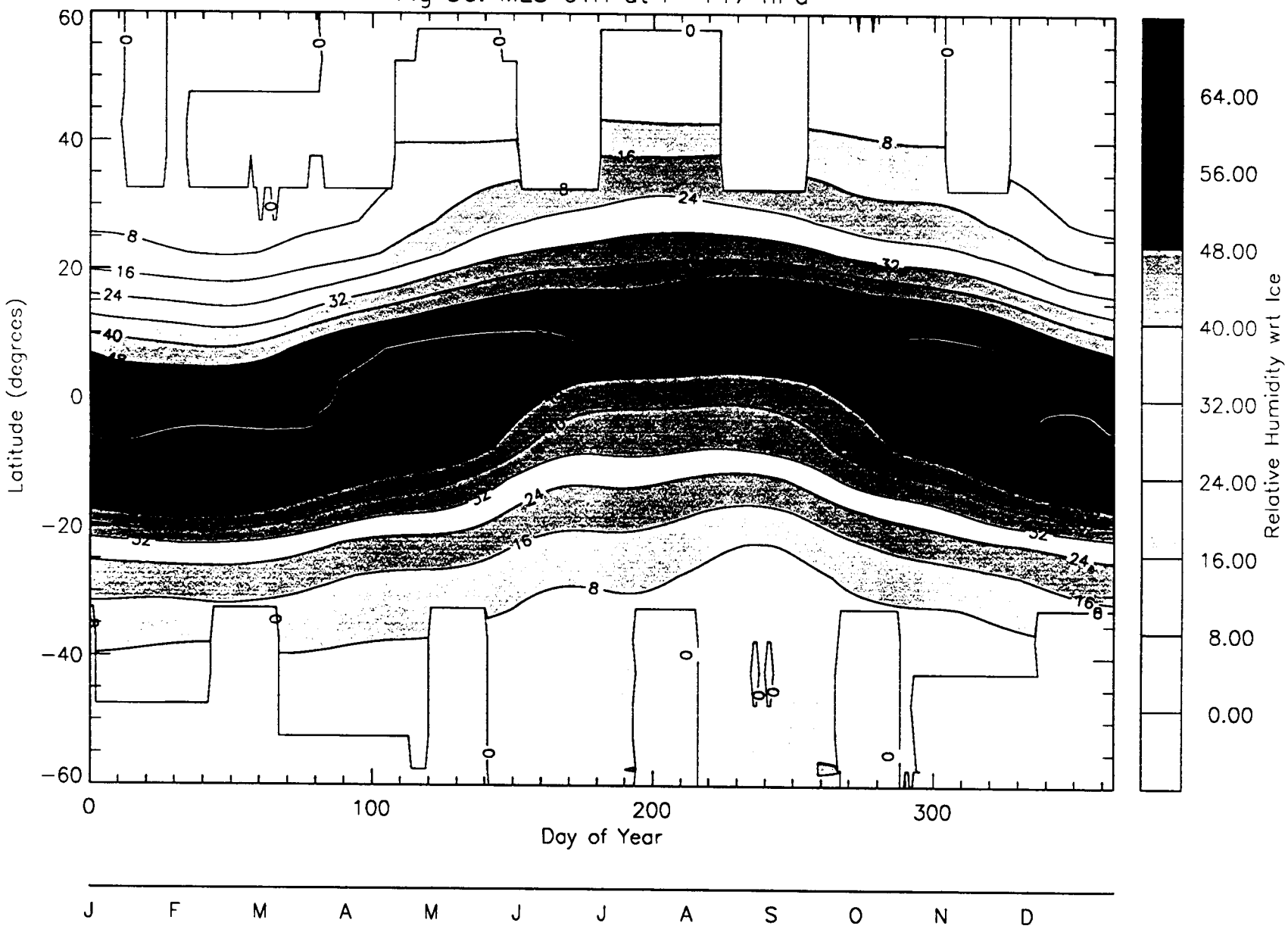
Fig 3a: MLS UTH at P=147 hPa
Latitude (degrees)
60
40
20
0
-20
-40
-60
0
100
200
300
Day of Year
J F M A M J J A S O N D
64.00
56.00
48.00
40.00
32.00
24.00
16.00
8.00
0.00
Relative Humidity wrt Ice

Fig 3b: MLS UTH at P=215 hPa

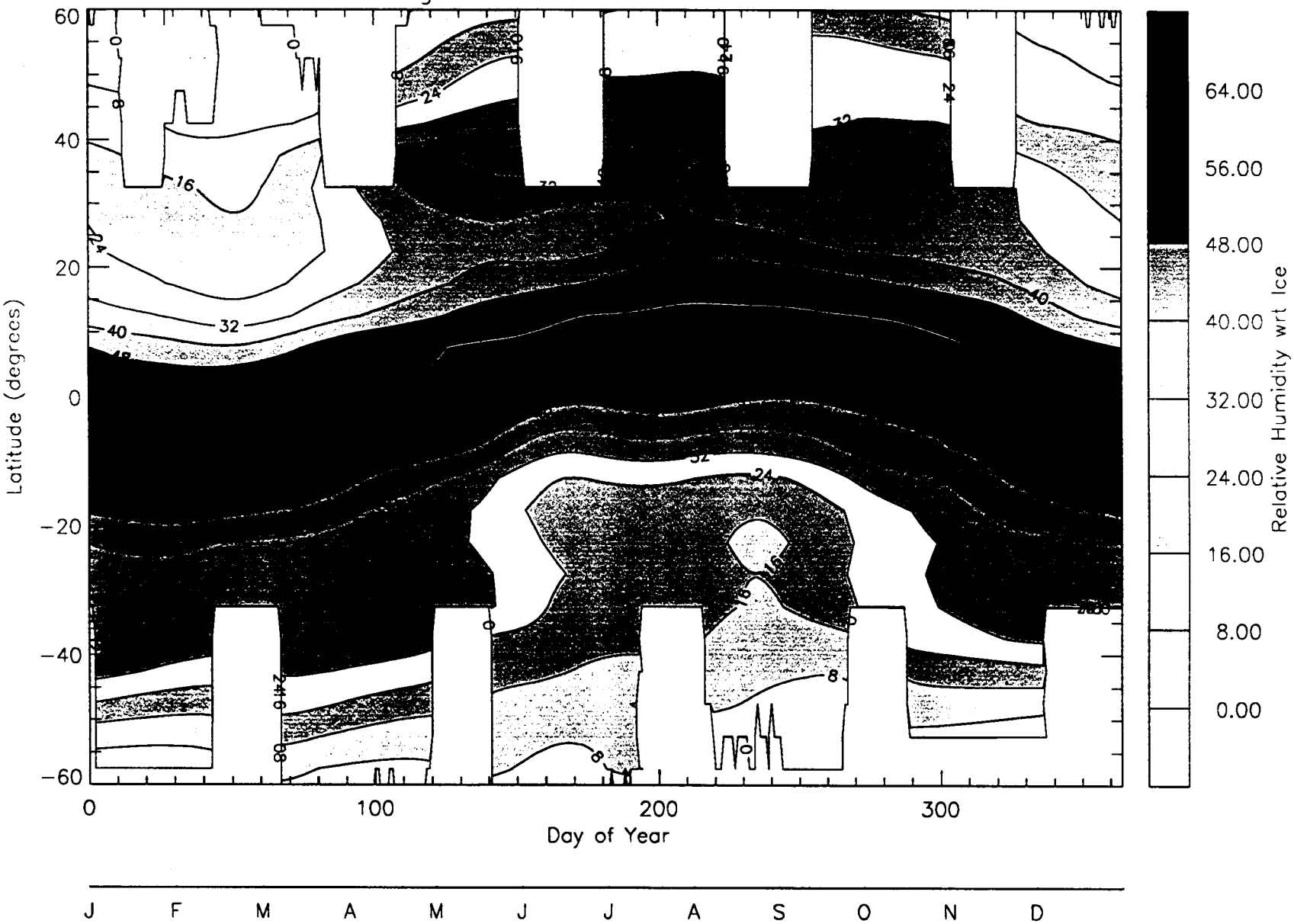

Fig 3c: MLS UTH at P=316 hPa

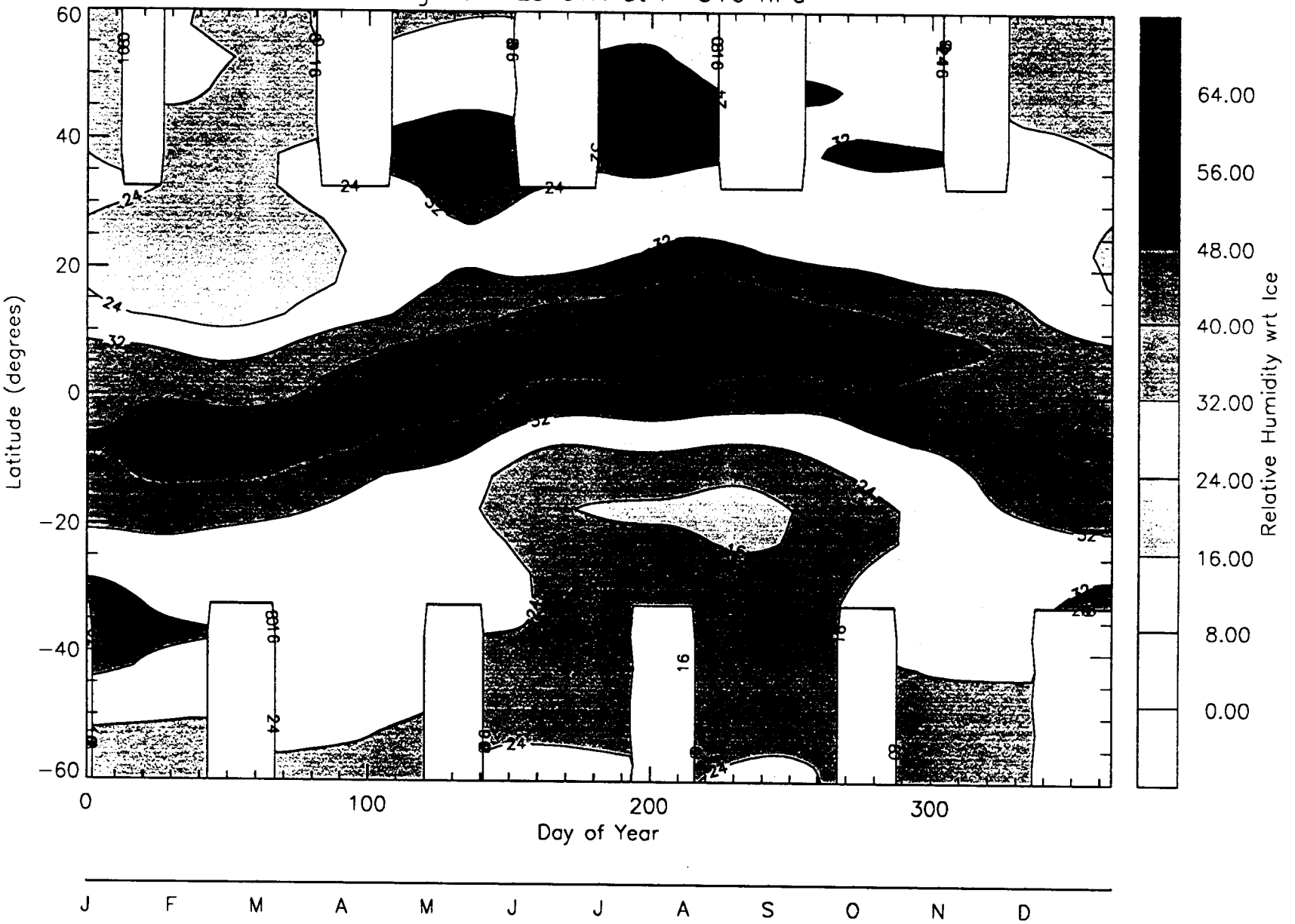

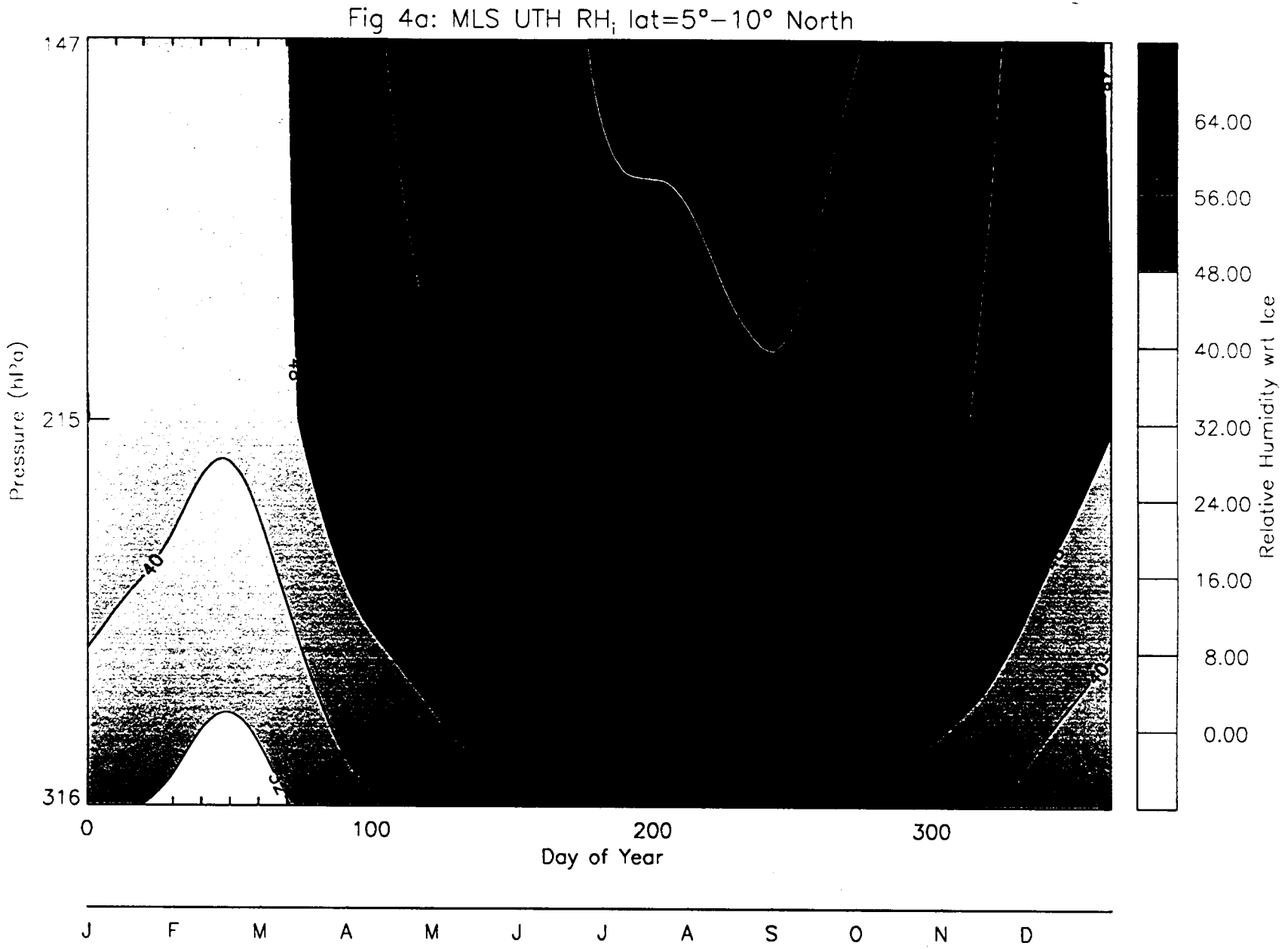
Fig 4a: MLS UTH RH$_i$ lat=5°–10° North
147
215
316
Pressure (hPa)
0
100
200
300
Day of Year
J
F
M
A
M
J
J
A
S
O
N
D
64.00
56.00
48.00
40.00
32.00
24.00
16.00
8.00
0.00
Relative Humidity wrt Ice

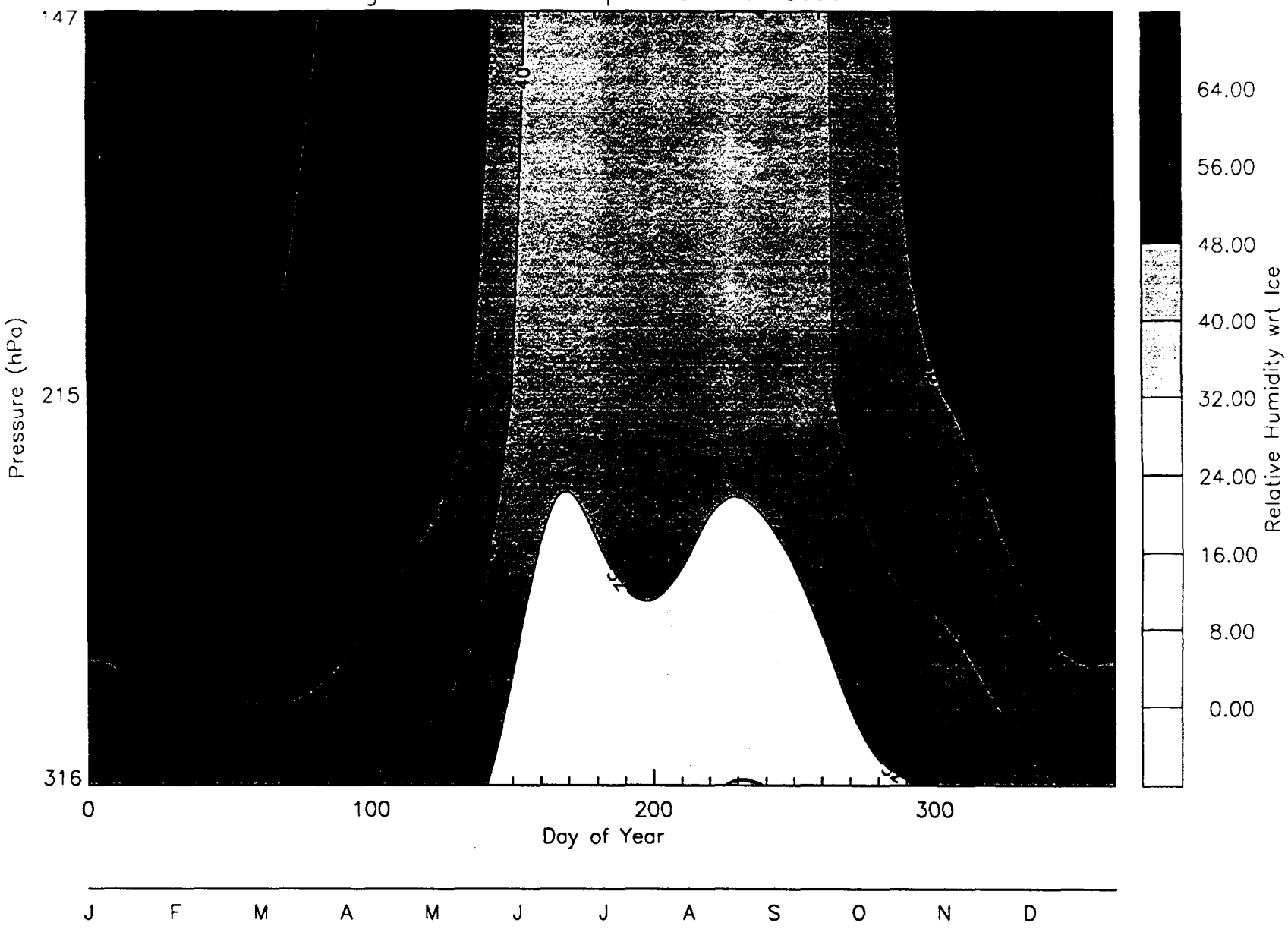
Fig 4b: MLS UTH RH$_i$ lat=5°–10° South
147
215
316
Pressure (hPa)
0
100
200
300
Day of Year
J
F
M
A
M
J
J
A
S
O
N
D
64.00
56.00
48.00
40.00
32.00
24.00
16.00
8.00
0.00
Relative Humidity wrt Ice

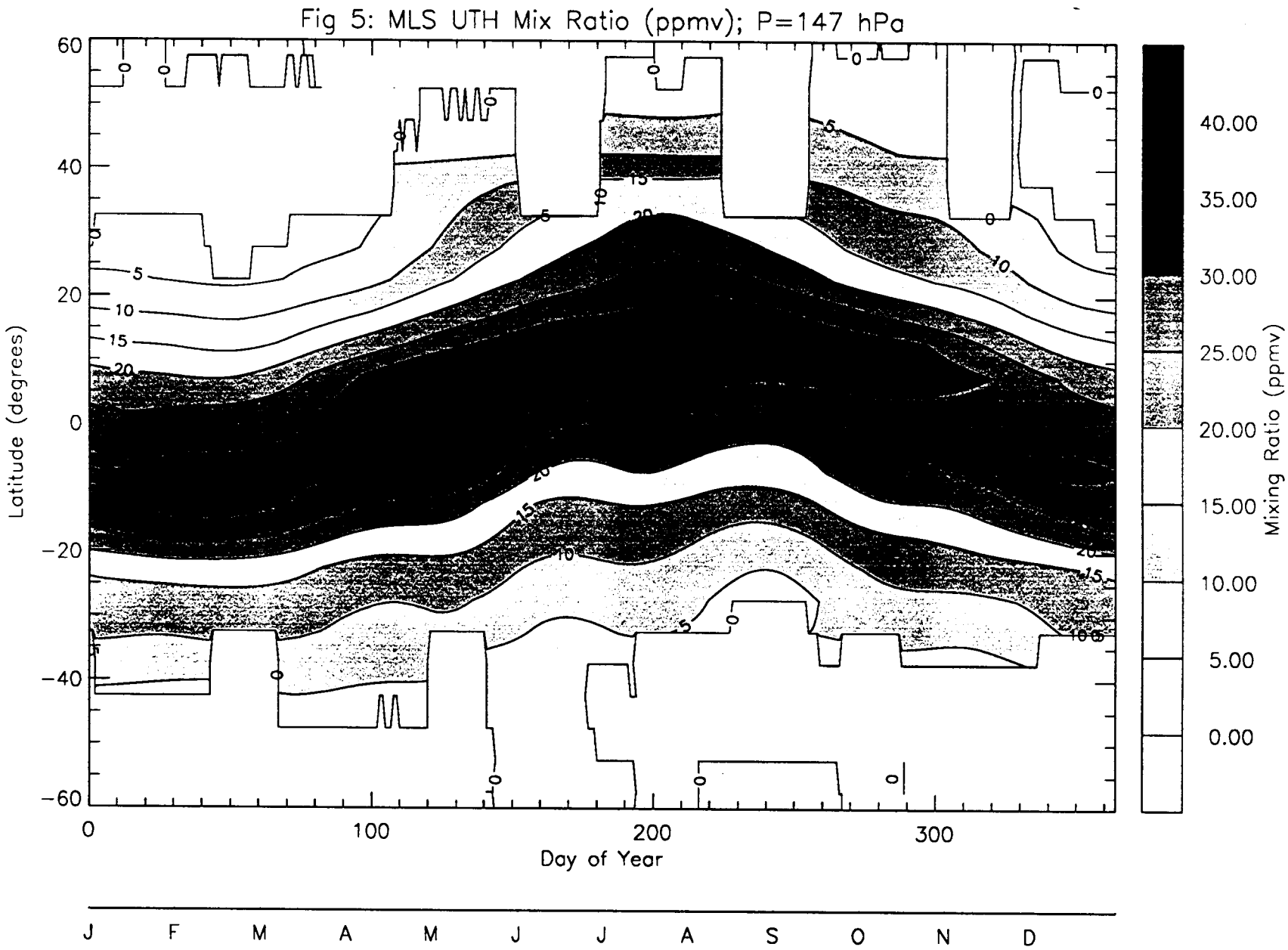
Fig 5: MLS UTH Mix Ratio (ppmv); P=147 hPa
Latitude (degrees)
60
40
20
0
-20
-40
-60
0
100
200
300
Day of Year
J F M A M J J A S O N D
Mixing Ratio (ppmv)
40.00
35.00
30.00
25.00
20.00
15.00
10.00
5.00
0.00

Fig. 6: 30S–30N Frequency Distribution

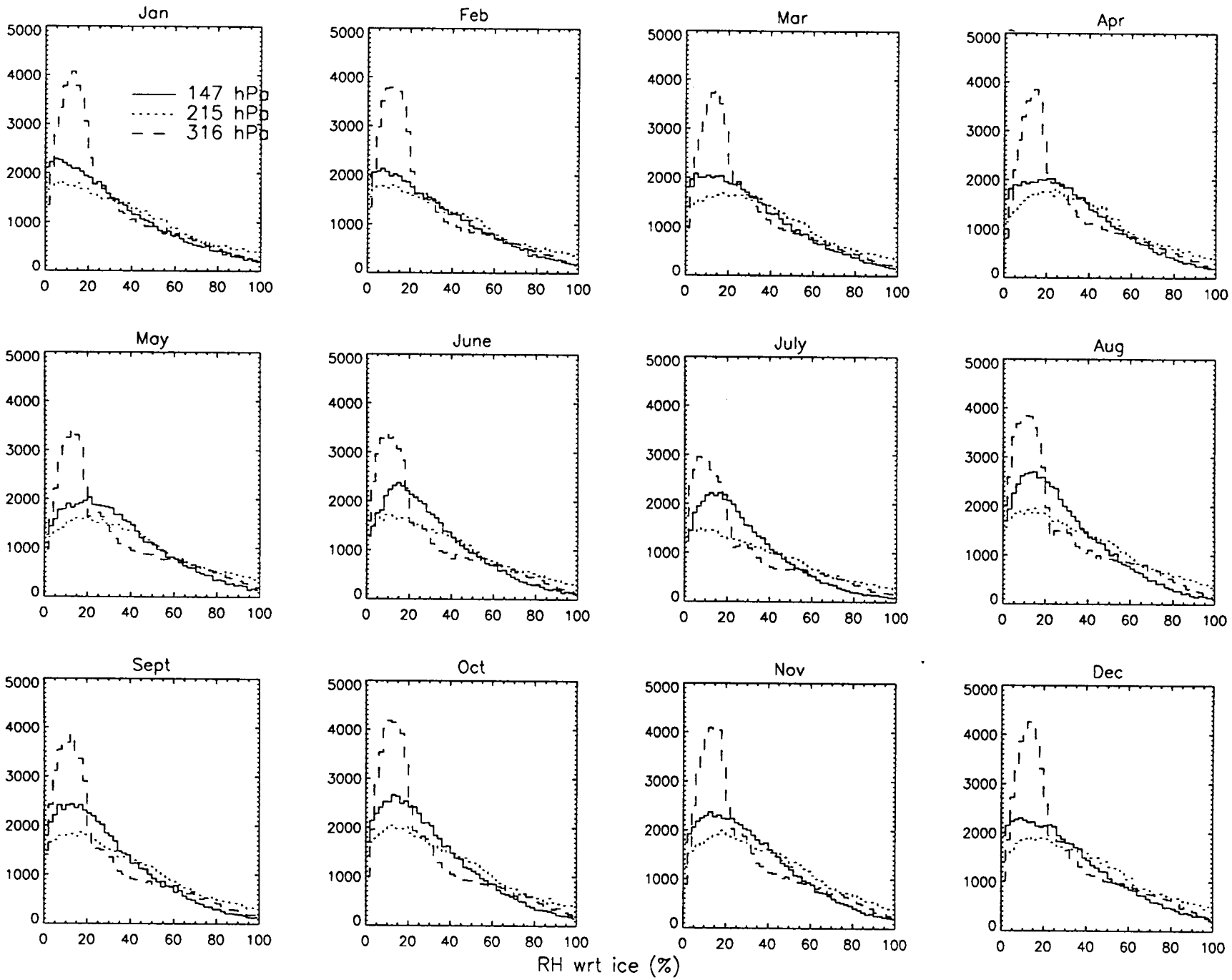

fig 7a: Mean

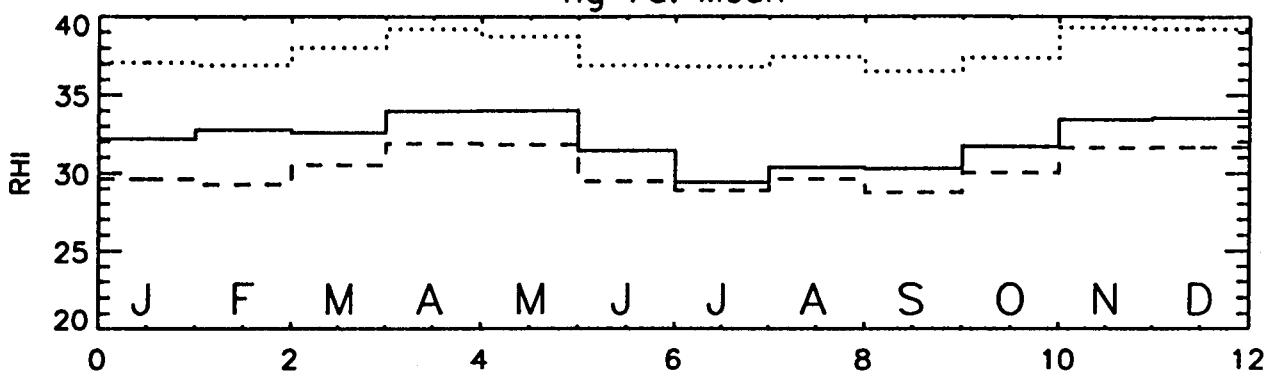


fig 7b: Median

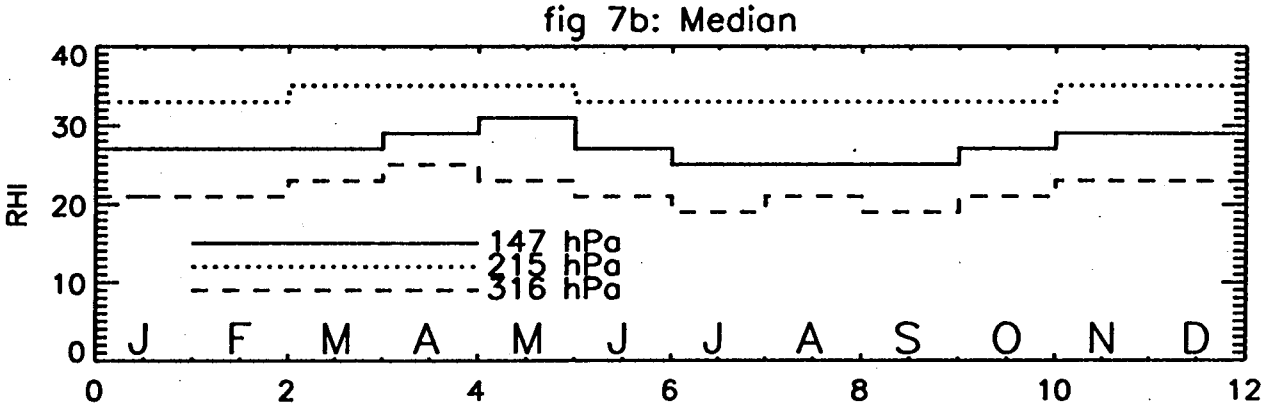


fig 7c: Mode